




Υ and η_b nuclear bound statesJ. J. Cobos-Martínez ^{1,*}, G. N. Zeminiani ² and K. Tsushima ²¹*Departamento de Física, Universidad de Sonora, Boulevard Luis Encinas J. y Rosales, Colonia Centro, Hermosillo, Sonora 83000, Mexico*²*Laboratório de Física Teórica e Computacional, Universidade Cidade de São Paulo (UNICID), 01506-000, São Paulo, SP, Brazil*

(Received 14 January 2022; accepted 1 February 2022; published 16 February 2022)

Υ and η_b nuclear bound-state energies are calculated for various nuclei, neglecting any possible effects of the widths. Essential input for the calculations, namely, the medium-modified B and B^* meson masses, as well as the density distributions in nuclei, are calculated within the quark-meson coupling (QMC) model. The attractive potentials for the Υ and η_b mesons in nuclei are calculated from the mass shifts of these mesons in nuclear matter in the local density approximation. These potentials originate from the in-medium enhanced BB and BB^* loops in their respective self-energy. After an extensive analysis we conclude that our results suggest that the Υ and η_b mesons should form bound states with all the nuclei considered.

DOI: [10.1103/PhysRevC.105.025204](https://doi.org/10.1103/PhysRevC.105.025204)**I. INTRODUCTION**

Quantum chromodynamics (QCD) is the accepted theory of the strong interactions at the fundamental level. However, a quantitative understanding of the strong force and strongly interacting matter from the underlying theory is still limited. The study of the interactions between heavy quarkonia and atomic nuclei is an important tool to gain an understanding of the strongly-interacting-matter properties in vacuum and extreme conditions of temperature and density based on QCD.

Since heavy quarkonium and nucleons do not share light (u , d) quarks [the Okubo-Zweig-Iizuka (OZI) rule suppresses the interactions mediated by the exchange of mesons made of only light quarks], heavy quarkonium interacts with nucleon primarily via gluons and therefore the production of heavy quarkonium in a nuclear medium can be of great relevance to explore the role played by gluons. If such states are indeed found experimentally to be bound to nuclei, it is therefore important to search for other sources of attraction which could lead to the binding of heavy quarkonium to nuclei. The binding of heavy quarkonium to nuclei may give evidence that the masses of these heavy mesons decrease in a nuclear medium.

Since the early work of Brodsky [1] that charmonium states may be bound to nuclei, a large amount of research, looking for alternatives to the light-meson exchange mechanism, has accumulated over the years to investigate the possible existence of such exotic states [2–24]. In addition to these, lattice QCD simulations for charmonium-nucleon interaction in free space were performed in the last decade [25–29]. Furthermore, more recently, studies for the binding of charmonia with nuclear matter and finite nuclei, as well as light mesons and baryons, were performed in lattice QCD simulations [30,31], albeit with unphysically heavy pion masses.

On the experimental side, the 12 GeV upgrade at the Jefferson Lab has made it possible to produce low-momentum heavy-quarkonia in an atomic nucleus. Recently [32], a photon beam was used to produce a J/Ψ meson near-threshold, which was identified by the decay into an electron-positron pair. Furthermore, with the construction of the FAIR facility in Germany, heavy and heavy-light mesons will be produced copiously by the annihilation of antiprotons on nuclei [33]. Experimental studies on η_c production in heavy-ion collisions at the LHC were performed in Refs. [34–38]. However, nearly no experiments have yet been aimed to produce the η_c at lower energies and its binding to nuclei, perhaps hinting at the difficulty to produce and detect such states. In the case of bottomonium, studies were made for Υ photoproduction at the Electron-Ion Collider [39,40], Υ production in p Pb collisions [41], and $\Upsilon(nl)$ (excited state) decay into $B^{(*)}\bar{B}^{(*)}$ [42]. With studies like these on heavy quarkonium and future planned ones, we will improve our understanding of the strong force and strongly interacting matter.

Returning to the phenomenological studies, the interactions frequently considered between the heavy quarkonium and the nuclear medium are the so-called QCD van der Waals (multigluon exchange) interactions [6,18–24]. One might think that this must be the case, since heavy quarkonium has no light quarks, whereas the nuclear medium is composed of light quarks, and thus the exchange of mesons composed of light quarks do not occur at the lowest order.

However, another possible mechanism, which we consider in this paper, for the heavy quarkonium to interact with the nuclear medium is through the excitation of the intermediate-state hadrons which do contain light quarks (B and B^* in this work). There is a great amount of evidence that the properties of hadrons change in medium [7,8,43,44] and this must be taken into account when addressing, for example, charmonium in nuclei. For instance, Refs. [7,8] have shown that the effect of the nuclear mean fields on the intermediate DD state is crucial when considering the J/Ψ interactions with atomic

*Corresponding author: jesus.cobos@fisica.uson.mx

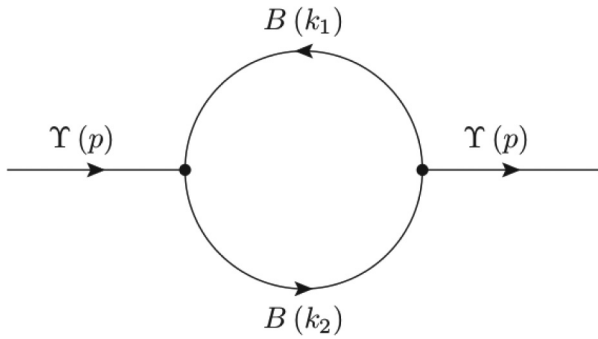


FIG. 1. BB meson loop contribution to the Υ self-energy.

nuclei. The modifications driven by the strong nuclear mean fields on the D mesons' light-quark component enhanced the self-energy such that it provides attraction to the J/Ψ . Furthermore, only recently the in-medium properties of η_c meson were renewed theoretically [45] using this mechanism.

In a recent paper [46], we estimated the mass shifts of the Υ and η_b mesons by considering the excitations of intermediate-state hadrons with light quarks in their self-energy. The estimates were made using an SU(5) effective Lagrangian density which contains both the Υ and η_b mesons with one universal coupling constant, and an anomalous coupling that respects SU(5) symmetry in the coupling constant. After expansion of the SU(5) effective Lagrangian with minimal substitutions, we obtained the interaction Lagrangians for calculating the BB and B^*B^* meson loops contributions to the Υ and η_b self-energies. As an example we show in Fig. 1 the BB meson loop contribution for the Υ self-energy.

For the study of the heavy quarkonium (Υ and η_b) interaction with the nuclear medium through the excitation of the intermediate-state hadrons we need to have knowledge of the in-medium properties of the B and B^* mesons, in particular their medium-modified masses. For this we used the quark-meson coupling (QMC) model [47], which has been successfully applied for various studies in nuclear matter and nuclei [5,7,48–55].

In Ref. [46] we did a study of the BB , BB^* , and B^*B^* meson loop contributions to the Υ self-energy in nuclear matter neglecting for the moment any possible imaginary part. After a detailed analysis, our predictions for the Υ and η_b mass shifts were given by including only the lowest-order BB meson loop contribution for the Υ , and only the BB^* meson loop contribution for the η_b , where the in-medium masses of the B and B^* mesons were calculated by the QMC model. We note that the in-medium B^* meson mass was calculated for the first time in Ref. [46]. In this work, we apply the mechanism described above by first extending our results in nuclear matter to finite nuclei and then considering the interactions between the Υ and η_b mesons and a wide mass range of atomic nuclei.

This article is organized as follows. In Sec. II we summarize the computational procedure used and discuss our results for the mass shifts of the Υ and η_b mesons in nuclear matter. These results indicate that nuclear medium provides attraction to these mesons and therefore in Sec. III we consider the nuclear bound states for the Υ and η_b mesons when these

mesons are produced nearly at rest inside a nucleus. Finally, in Sec. IV we give a summary and conclusions.

II. MASS SHIFTS IN NUCLEAR MATTER

In this section we summarize the results obtained for the mass shifts of the Υ and η_b mesons in nuclear matter. The details of this analysis can be found in Ref. [46].

A. Υ mass shift

The Υ mass shift in nuclear matter originates from the modifications of the BB , BB^* , and B^*B^* meson loops contributions to the Υ self-energy, relative to those in free space; see, for example, Fig. 1. The self-energy is calculated using effective SU(5)-flavor symmetric Lagrangians at the hadronic level [46,56] for the interaction vertices ΥBB , ΥB^*B^* , and ΥBB^* , neglecting any possible imaginary part. In Ref. [46] we made an extensive analysis of these contributions to the Υ self-energy and found that, for example, the B^*B^* loop gives an unexpectedly large contribution. For this reason, and to be consistent with the η_b case studied below, we decided to be conservative and consider only the BB loop contribution to the Υ self-energy, leaving for the future a full study. The interaction Lagrangian for the ΥBB vertex is given by

$$\mathcal{L}_{\Upsilon BB} = ig_{\Upsilon BB} \Upsilon^\mu [\bar{B} \partial_\mu B - (\partial_\mu \bar{B}) B], \quad (1)$$

where the following convention is adopted for the isospin doublets of the B mesons:

$$B = \begin{pmatrix} B^+ \\ B^0 \end{pmatrix}, \quad \bar{B} = (B^- \quad \bar{B}^0).$$

The coupling constant $g_{\Upsilon BB}$ for the vertex ΥBB is calculated from the experimental data for $\Gamma(\Upsilon \rightarrow e^+e^-)$ using the vector-meson dominance model. This gives $g_{\Upsilon BB} = 13.2$; see Refs. [46,56] and references therein for details. A similar approach was taken in Refs. [7,57] to determine the coupling constant $g_{J/\Psi DD} = 7.64$ for the vertex $J/\Psi DD$.

Including only the BB loop, Eq. (1), the Υ self-energy Σ_Υ is given by

$$\Sigma_\Upsilon(k^2) = -\frac{g_{\Upsilon BB}^2}{3\pi^2} \int_0^\infty dq q^2 I(q^2) \quad (2)$$

for an Υ at rest, where

$$I(q^2) = \frac{1}{\omega_B} \left(\frac{q^2}{\omega_B - m_\Upsilon^2/4} \right), \quad (3)$$

and $\omega_B = (q^2 + m_B^2)^{1/2}$. The integral in Eq. (2) is divergent and therefore needs to be regularized. To do this, we introduce into the integrand of Eq. (2) a phenomenological vertex form factor

$$u_B(q^2) = \left(\frac{\Lambda_B^2 + m_\Upsilon^2}{\Lambda_B^2 + 4\omega_B^2(q^2)} \right)^2, \quad (4)$$

with cutoff parameter Λ_B [7–10,58–62] for each ΥBB vertex. In a later section we discuss the non-negligible role played by this form factor and the cutoff parameter Λ_B . For the moment, we point out that form factors are necessary to take into account the finite size of the mesons participating in the

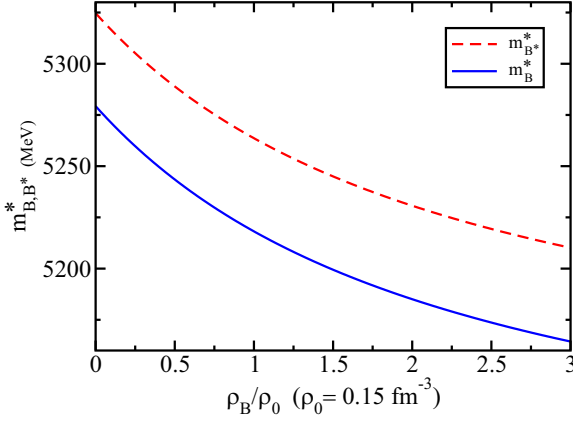


FIG. 2. B and B^* meson effective Lorentz-scalar masses in symmetric nuclear matter versus baryon density.

vertices, while the cutoff Λ_B , which is an unknown input to our calculation, may be associated with energies needed to probe the internal structure of the mesons; see Ref. [46] for a more extensive discussion. Thus, in order to reasonably include these effects and to quantify the sensitivity of our results to its value, we vary Λ_B over the interval 2000–6000 MeV.

The Υ mass shift in nuclear matter Δm_Υ is computed from the difference between its in-medium mass m_Υ^* and its value in vacuum, m_Υ , namely,

$$\Delta m_\Upsilon = m_\Upsilon^* - m_\Upsilon, \quad (5)$$

where these masses are computed self-consistently from

$$m_\Upsilon^2 = (m_\Upsilon^0)^2 + \Sigma_\Upsilon(k^2 = m_\Upsilon^2), \quad (6)$$

where m_Υ^0 is the bare Υ mass and the Υ self-energy $\Sigma_\Upsilon(k^2)$ is given in Eq. (2). The Λ_B -dependent Υ bare mass, m_Υ^0 , is fixed such that we reproduce the physical Υ mass, namely $m_\Upsilon = 9640$ MeV.

The in-medium Υ mass is obtained by solving Eq. (6) with the self-energy calculated with the medium-modified B mass, which was calculated in Ref. [46], together with that for the B^* meson, using the quark-meson coupling model (QMC) as a function of the nuclear matter density ρ_B . The results obtained in this way are presented in Fig. 2 and show that the QMC model gives a similar downward mass shift for the B and B^* in symmetric nuclear matter. For example, at the saturation density $\rho_0 = 0.15 \text{ fm}^{-3}$, the mass shifts for the B and B^* mesons are, respectively, $(m_B^* - m_B) = -61$ MeV and $(m_{B^*}^* - m_{B^*}) = -61$ MeV, where the difference in their mass shift values appears in the next digit. The values for the masses in vacuum for the B and B^* mesons used are $m_B = 5279$ MeV and $m_{B^*} = 5325$ MeV, respectively.

The nuclear density dependence of the Υ mass is driven by the intermediate BB state interactions with the nuclear medium, where the effective scalar- and vector-meson mean fields couple to the light u and d quarks in the bottom mesons. In Fig. 3 we show the results for the Υ mass shift as a function of the nuclear matter density ρ_B , for five values of the cutoff parameter Λ_B . As can be seen from Figs. 2 and 3, a decreasing B meson mass in-medium induces a negative mass shift for the Υ . This happens because a decrease of the B meson mass

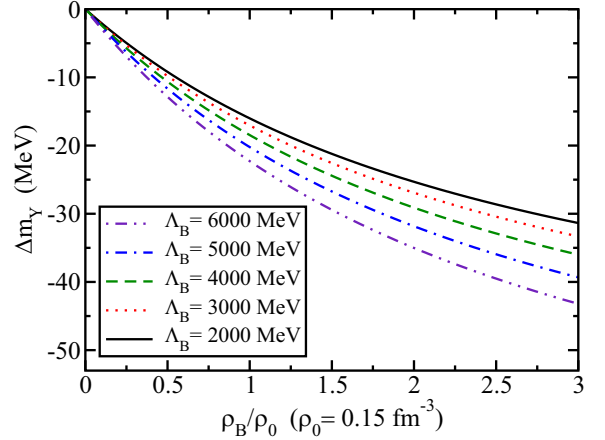


FIG. 3. Υ mass shift in nuclear matter as a function of the nuclear matter density ρ_B .

enhances the BB meson loop contribution in nuclear matter relative to that in vacuum. Expectedly, the mass shift of the Υ is dependent on the value of the cutoff mass Λ_B used, being larger for larger Λ_B ; see Ref. [46] for further details. For example, for the values of the cutoff shown in Fig. 3, the Υ mass shift varies from -16 to -22 MeV at $\rho_B = \rho_0$.

B. η_b mass shift

For the calculation of the η_b mass shift in nuclear matter, we proceed similarly to the Υ case and take into account only the BB^* loop contribution to the η_b self-energy. In Ref. [46] we have also studied the inclusion of the $\eta_b B^* B^*$ interaction in the η_b self-energy and found that its contribution to the mass shift is essentially negligible. Thus, in order to be consistent with the Υ case above, i.e., in both cases we consider only the minimal contribution, here we only give results for the BB^* loop in the η_b self-energy. The effective Lagrangian for the $\eta_b BB^*$ interaction is

$$\begin{aligned} \mathcal{L}_{\eta_b BB^*} = & ig_{\eta_b BB^*} [(\partial^\mu \eta_b)(\bar{B}_\mu^* B - \bar{B} B_\mu^*) \\ & - \eta_b (\bar{B}_\mu^* (\partial^\mu B) - (\partial^\mu \bar{B}) B_\mu^*)], \end{aligned} \quad (7)$$

where $g_{\eta_b BB^*}$ is the coupling constant for the $\eta_b BB^*$ vertex. We use its value in the SU(5) scheme [46], namely,

$$g_{\eta_b BB^*} = g_{\Upsilon BB} = g_{\Upsilon B^* B^*} = \frac{5g}{4\sqrt{10}}. \quad (8)$$

Using Eq. (7), the η_b self-energy for an η_b at rest is given by [45]

$$\Sigma_{\eta_b} = \frac{8g_{\eta_b BB^*}^2}{\pi^2} \int_0^\infty dq q^2 K(\mathbf{q}^2), \quad (9)$$

where

$$\begin{aligned} K(\mathbf{q}^2) = & \frac{m_{\eta_b}^2 (-1 + q_0^2/m_{B^*}^2)}{(q_0^2 - \omega_{B^*}^2)(q_0 - m_{\eta_b} - \omega_B)} \Big|_{q_0=m_{\eta_b}-\omega_B} \\ & + \frac{m_{\eta_b}^2 (-1 + q_0^2/m_{B^*}^2)}{(q_0 - \omega_{B^*})[(q_0 - m_{\eta_b})^2 - \omega_B^2]} \Big|_{q_0=-\omega_{B^*}}, \end{aligned} \quad (10)$$

and $\omega_{B^*} = (\mathbf{q}^2 + m_{B^*}^2)^{1/2}$.

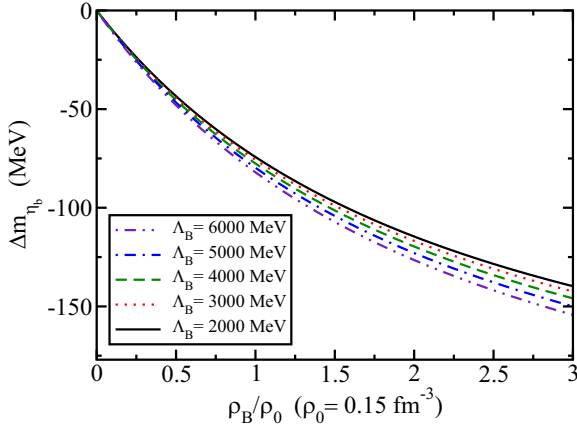


FIG. 4. η_b mass shift in nuclear matter as a function of the nuclear matter density ρ_B .

The mass of the η_b meson, in vacuum and in nuclear matter, is computed similarly to the Υ case. First, we introduce form factors, as in Eq. (4), into each $\eta_b BB^*$ vertex, with $\Lambda_B = \Lambda_{B^*}$, in order to regularize the divergent integral in the self-energy, Eq. (9). Second, we fix the value of the η_b bare mass using the physical (vacuum) mass of the η_b , namely, $m_{\eta_b} = 9399$ MeV, using Eq. (6) appropriately written for the η_b case. Then, for the calculation of the η_b mass shift in nuclear matter, the self-energy Σ_{η_b} is computed using the medium-modified B and B^* masses calculated in the QMC model and shown in Fig. 2. The results for the η_b mass shift in nuclear matter are shown in Fig. 4 as a function of the nuclear matter density ρ_B . Note that we use the same range of values for the cutoff mass Λ_B as for the Υ . As can be seen from Fig. 4, the mass of the η_b is shifted downwards in nuclear matter for all values of the cutoff Λ_B , similarly to the Υ . For example, at the normal density of nuclear matter ρ_0 , the mass shift varies from -75 to -82 MeV when the cutoff varies from $\Lambda_B = 2000$ MeV to $\Lambda_B = 6000$ MeV. Similarly to the Υ mass shift, the dependence of the η_b mass shift on the values of the cutoff is small, for example, just -7 MeV when the cutoff is increased by a factor of three at $\rho_B = \rho_0$.

C. Discussion of the Υ and η_b mass-shift results

Surprisingly, the mass shift for the η_b is larger than that of the Υ for the same range of cutoff values explored; see Figs. 3 and 4. A similar difference in mass shifts was observed for the J/Ψ and η_c mesons in Refs. [7,45] using the corresponding Lagrangians in the SU(4) flavor sector. As demonstrated in Refs. [45,46], these differences in the mass shifts for the η_b and Υ are probably due to the following reasons: (a) a badly broken SU(5) symmetry such that the couplings $g_{\eta_b BB^*}$ and $g_{\Upsilon BB}$ are very different, and not equal as assumed here, see Eq. (8). Indeed, as shown in Ref. [45], the mass shift for the η_c gets closer to that of the J/Ψ when SU(4) flavor symmetry is broken, such that $g_{\eta_c DD^*} = (0.6/\sqrt{2}) g_{J/\Psi DD} \simeq 0.424 g_{J/\Psi DD}$ [45,63]. SU(5) flavor symmetry, like SU(4), is also broken in nature, as attested to by the difference in masses of the Υ and η_b mesons. However, since we do not have an empirical value

for $g_{\eta_b BB^*}$, which we can use to compute the η_b self-energy, we therefore resort to SU(5) symmetry and use the value for $g_{\eta_b BB^*}$ given in Eq. (8). (b) The form factors are not equal for the vertices ΥBB and $\eta_b BB^*$ and we have to readjust the cutoff values, which means $\Lambda_B \neq \Lambda_{B^*}$ and the comparisons for the mass shifts have to be made for different values of the cutoffs. This is also a reason why we explore a range of values for Λ_B . (c) At the $g_{\eta_b BB^*}^2$ order, the number of possible contractions to give the BB^* loop in the η_b self-energy is $4 \times 4 = 16$ for the isodoublet B and B^* fields, and this number is larger than that of $2 \times 2 = 4$ to give the BB loop in the Υ self-energy at the $g_{\Upsilon BB}^2$ order [see Eqs. (1) and (7)]. This may give the larger contribution for the η_b potential.

The results for the mass shifts in nuclear matter, shown in Figs. 3 and 4, for the Υ and η_b , respectively, support the argument that the nuclear medium provides attraction to these mesons and open the possibility to study the binding of these mesons to nuclei since the mass shifts, for both the Υ and η_b , at around $\rho_B = \rho_0$, are significant. We will see in the next section that this is indeed the case and allows for the formation of nuclear bound states for both the Υ and η_b , and furthermore we calculate the corresponding binding energies for several nuclei.

III. NUCLEAR BOUND STATES

The results for the mass shifts of the Υ and η_b in nuclear matter clearly indicate that nuclear medium provides attraction to these mesons. Therefore, we now consider the nuclear bound states of the Υ and η_b mesons when these mesons have been produced nearly at rest inside nucleus A and study the following nuclei in a wide range of masses, namely ${}^4\text{He}$, ${}^{12}\text{C}$, ${}^{16}\text{O}$, ${}^{40}\text{Ca}$, ${}^{48}\text{Ca}$, ${}^{90}\text{Zr}$, ${}^{197}\text{Au}$, and ${}^{208}\text{Pb}$.

In the local density approximation, the bottomonium h ($h = \Upsilon, \eta_b$) potential within nucleus A is given by

$$V_{hA}(r) = \Delta m_h(\rho_B^A(r)), \quad (11)$$

where r is the distance from the center of the nucleus and Δm_h is the mass shift computed in Sec. II for $h = \Upsilon, \eta_b$. The nuclear density distributions $\rho_B^A(r)$ for the nuclei listed above are calculated using the QMC model [51], except for ${}^4\text{He}$, which we obtain from Ref. [64].

In Figs. 5 and 6 we present the bottomonium h -nucleus potentials for the eight nuclei mentioned above and the same values of the cutoff parameter Λ_B that were used in the computation of the mass shifts in Sec. II. We can see from Figs. 5 and 6 that the V_{hA} potentials, for $h = \Upsilon$ and η_b , respectively, are attractive for all nuclei and all values of the cutoff mass parameter. However, for each nuclei, the depth of the potential depends on the value of the cutoff parameter, being more attractive the larger Λ_B is. This dependence is expected and is, indeed, an uncertainty in the results obtained in our approach.

We now compute the bottomonium h -nucleus bound-state energies for the potentials shown in Figs. 5 and 6 by solving the Klein-Gordon equation for these potentials. To apply the Klein-Gordon equation to obtain the Υ -nucleus single-particle energies, since the Υ is a spin-1 particle, we make an approximation where the transverse and longitudinal components in the Proca equation are expected to be very similar

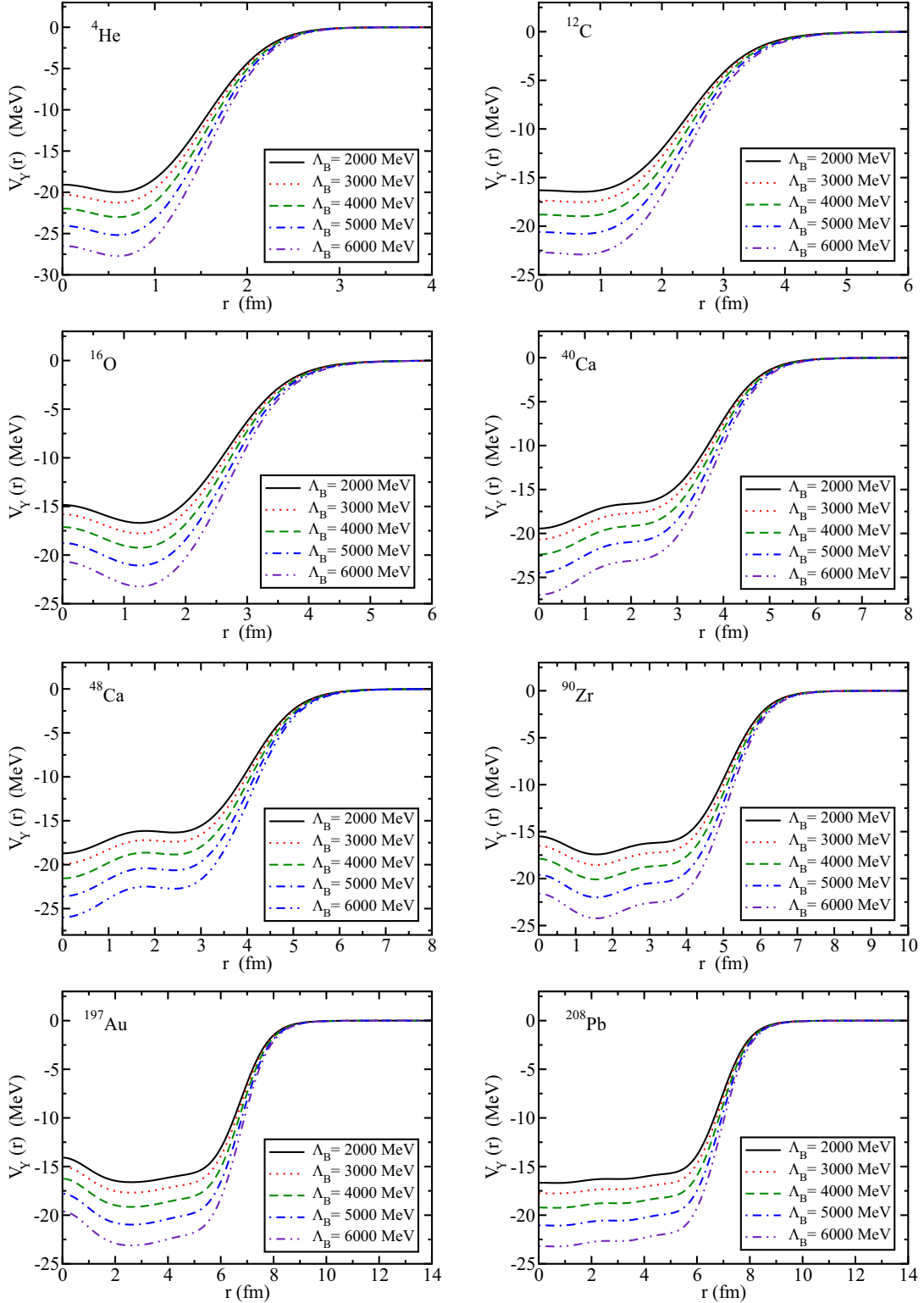


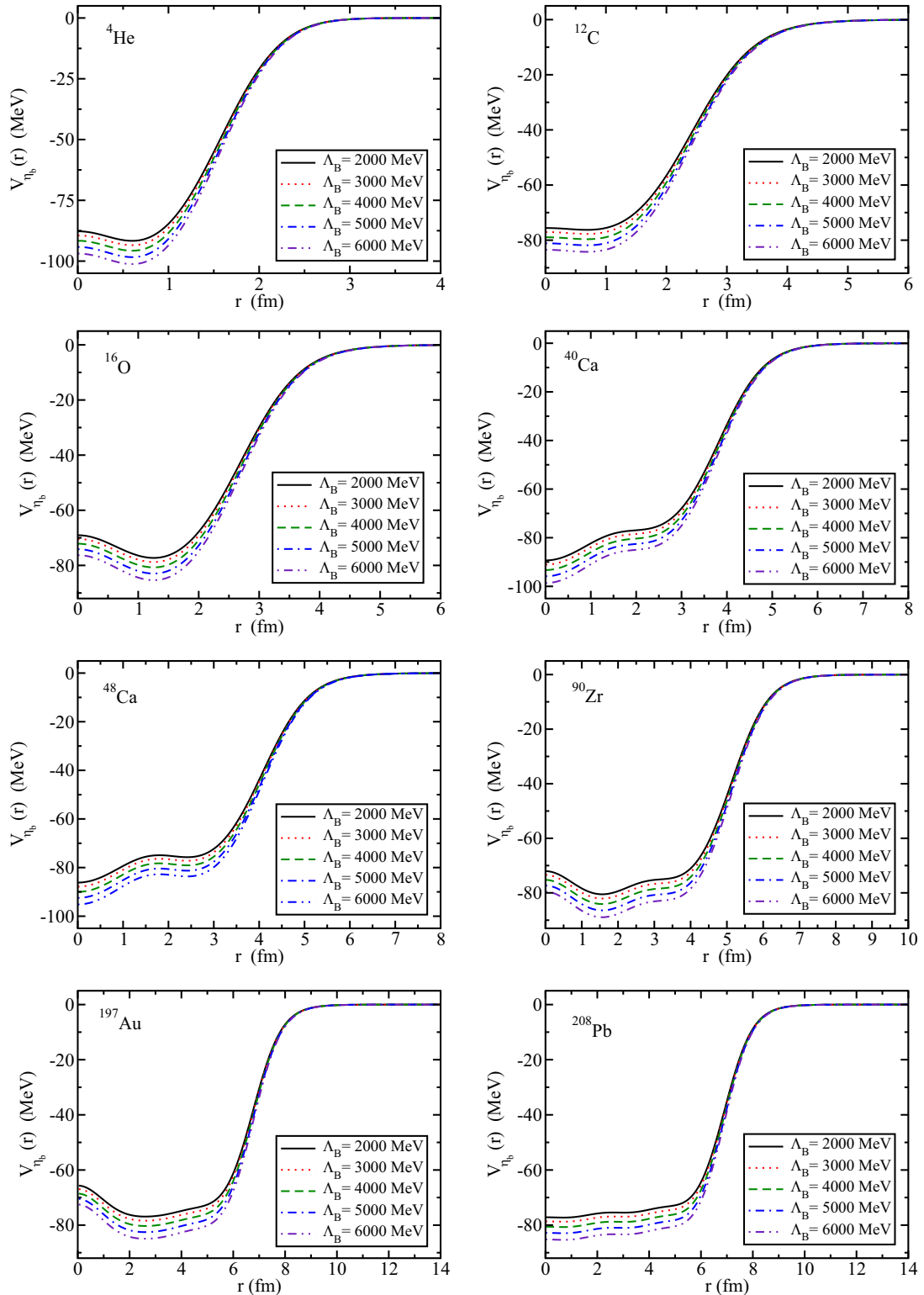
FIG. 5. Υ -nucleus potentials for various nuclei and values of the cutoff parameter Λ_B .

for an Υ at rest, hence it is reduced to one component, which corresponds to the Klein-Gordon equation.

We treat the bottomonium h -nucleus potential as a scalar and add it to the mass term in the Klein-Gordon

equation

$$\{-\nabla^2 + [m + V_{hA}(\vec{r})]^2\}\phi_h(\vec{r}) = \mathcal{E}^2\phi_h(\vec{r}), \quad (12)$$


 FIG. 6. η_b -nucleus potentials for various nuclei and values of the cutoff parameter Λ_B .

where $h = \Upsilon, \eta_b$, $m = m_h m_A / (m_h + m_A)$ is the reduced mass of the bottomonium h -nucleus system with m_h (m_A) the mass of bottomonium h (nucleus A) in vacuum, and $V_{hA}(\vec{r})$ is the bottomonium h -nucleus potential given in Eq. (11) and shown in Figs. 5 and 6.

We note that in previous works we have approximated Eq. (12) by ignoring the V_{hA}^2 term. We now solve the full Klein-Gordon equation Eq. (12) using momentum-space methods. Here, the Klein-Gordon equation is first converted to a momentum-space representation via a Fourier transform,

TABLE I. Bound-state energies of Υ in nucleus of mass number A . All dimensioned quantities are in MeV.

		Bound-state energies				
$n\ell$		$\Lambda_B = 2000$	$\Lambda_B = 3000$	$\Lambda_B = 4000$	$\Lambda_B = 5000$	$\Lambda_B = 6000$
${}^4_{\Upsilon}\text{He}$	1s	-5.6	-6.4	-7.5	-9.0	-10.8
${}^{12}_{\Upsilon}\text{C}$	1s	-10.6	-11.6	-12.8	-14.4	-16.3
	1p	-6.1	-6.8	-7.9	-9.3	-10.9
	1d	-1.5	-2.1	-2.9	-4.0	-5.4
	2s	-1.6	-2.1	-2.8	-3.8	-5.1
	1s	-11.9	-12.9	-14.2	-15.8	-17.8
${}^{16}_{\Upsilon}\text{O}$	1p	-8.3	-9.2	-10.4	-11.9	-13.7
	1d	-4.4	-5.1	-6.2	-7.5	-9.2
	2s	-3.7	-4.4	-5.4	-6.7	-8.3
	1f	n	-0.9	-1.8	-2.9	-4.3
	1s	-15.5	-16.6	-18.2	-20.0	-22.3
${}^{40}_{\Upsilon}\text{Ca}$	1p	-13.3	-14.4	-15.9	-17.7	-19.8
	1d	-10.8	-11.9	-13.3	-15.0	-17.1
	2s	-10.3	-11.3	-12.7	-14.4	-16.4
	1f	-8.1	-9.1	-10.4	-12.1	-14.0
${}^{48}_{\Upsilon}\text{Ca}$	1s	-15.3	-16.4	-17.9	-19.7	-21.8
	1p	-13.5	-14.6	-16.0	-17.8	-19.9
	1d	-11.4	-12.4	-13.8	-15.6	-17.6
	2s	-10.8	-11.8	-13.2	-14.9	-16.9
	1f	-9.1	-10.1	-11.4	-13.1	-15.0
${}^{90}_{\Upsilon}\text{Zr}$	1s	-15.5	-16.6	-18.1	-19.9	-22.0
	1p	-14.5	-15.5	-17.0	-18.8	-20.9
	1d	-13.2	-14.2	-15.7	-17.4	-19.5
	2s	-12.7	-13.8	-15.2	-16.9	-19.0
	1f	-11.7	-12.7	-14.1	-15.9	-17.9
${}^{197}_{\Upsilon}\text{Au}$	1s	-15.3	-16.3	-17.7	-19.4	-21.5
	1p	-14.7	-15.8	-17.2	-18.9	-20.9
	1d	-14.0	-15.0	-16.4	-18.1	-20.1
	2s	-13.7	-14.7	-16.0	-17.8	-19.8
	1f	-13.2	-14.2	-15.6	-17.3	-19.3
${}^{208}_{\Upsilon}\text{Pb}$	1s	-15.7	-16.8	-18.2	-20.0	-22.1
	1p	-15.2	-16.2	-17.7	-19.4	-21.5
	1d	-14.5	-15.5	-16.9	-18.7	-20.8
	2s	-14.1	-15.2	-16.6	-18.3	-20.4
	1f	-13.6	-14.7	-16.1	-17.8	-19.9

followed by a partial-wave decomposition. For a given value of angular momentum l , the eigenvalues \mathcal{E}_{nl} of the resulting equation are found by the inverse iteration eigenvalue algorithm.

The bound-state energies E of the bottomonium h -nucleus system, given by $E_{nl} = \mathcal{E}_{nl} - m$, are listed in Tables I and II. In Table I we show the Υ -nucleus bound state energies for all nuclei listed at the beginning of this section and the same range of values for the cutoff mass parameter as used in the mass-shift calculation. For each nucleus we have listed only a few bound states, since the number of bound states increases with the mass of the nucleus and for the heaviest of these the number of bound states is quite large. For example, for the heaviest nucleus we have ≈ 70 states. In Table II we show the η_b -nucleus bound-state energies for the same nuclei and range of values of the cutoff mass parameter as in Table I. Furthermore, as in the case of the case of the Υ -nucleus bound-state energies, for each nucleus we have listed only a few bound states. For the heaviest nucleus we have ≈ 200

states and clearly is not practical to show them all. We have also solved the Schrödinger equation for all the potentials shown in Figs. 5 and 6 and found essentially the same results. We can now give some general conclusion concerning the results given in Tables I and II. These results show that the Υ and η_b mesons are expected to form bound states with all the nuclei studied, independent of the value of the cutoff parameter Λ_B . However, the particular values for the bound-state energies are dependent on the cutoff parameter, increasing in absolute value as the cutoff parameter increases. This dependence was expected from the behavior of the bottomonium h -nucleus potentials, since these are more attractive for larger values of the cutoff parameter. Note also that bottomonium h binds more strongly to heavier nuclei and therefore a richer spectrum is expected for these nuclei.

Discussion of the Υ and η_b single-particle energies

The discussion of the mass shifts results for the Υ and η_b carried out in Sec. II C can be translated to the Υ and η_b

TABLE II. Bound-state energies of η_b in nucleus of mass number A . All dimensioned quantities are in MeV.

		Bound-state energies				
	$n\ell$	$\Lambda_B = 2000$	$\Lambda_B = 3000$	$\Lambda_B = 4000$	$\Lambda_B = 5000$	$\Lambda_B = 6000$
${}^4_{\eta_b}\text{He}$	1s	-63.1	-64.7	-66.7	-69.0	-71.5
	1p	-40.6	-42.0	-43.7	-45.8	-48.0
	1d	-17.2	-18.3	-19.7	-21.4	-23.2
	2s	-15.6	-16.6	-17.9	-19.4	-21.1
${}^{12}_{\eta_b}\text{C}$	1s	-65.8	-67.2	-69.0	-71.1	-73.4
	1p	-57.0	-58.4	-60.1	-62.1	-64.3
	1d	-47.5	-48.8	-50.4	-52.3	-54.4
	2s	-46.3	-47.5	-49.1	-51.0	-53.0
${}^{16}_{\eta_b}\text{O}$	1f	-37.5	-38.7	-40.2	-42.0	-43.9
	1s	-67.8	-69.2	-71.0	-73.1	-75.4
	1p	-61.8	-63.2	-64.9	-67.0	-69.2
	1d	-54.9	-56.2	-57.9	-59.9	-62.0
${}^{40}_{\eta_b}\text{Ca}$	2s	-53.2	-54.6	-56.3	-58.2	-60.3
	1f	-47.3	-48.6	-50.2	-52.1	-54.2
	1s	-79.0	-80.6	-82.6	-85.0	-87.5
	1p	-75.4	-77.0	-79.0	-81.4	-83.9
${}^{48}_{\eta_b}\text{Ca}$	1d	-71.4	-73.0	-74.9	-77.2	-79.7
	2s	-70.5	-72.0	-74.0	-76.3	-78.8
	1f	-67.0	-68.5	-70.4	-72.7	-75.1
	1s	-76.7	-78.2	-80.2	-82.5	-85.0
${}^{90}_{\eta_b}\text{Zr}$	1p	-74.0	-75.5	-77.4	-79.7	-82.1
	1d	-70.8	-72.3	-74.2	-76.4	-78.8
	2s	-69.9	-71.4	-73.3	-75.5	-77.9
	1f	-67.2	-68.6	-70.6	-72.8	-75.1
${}^{197}_{\eta_b}\text{Au}$	1s	-75.5	-77.0	-78.9	-81.1	-83.5
	1p	-74.1	-75.6	-77.5	-79.7	-82.1
	1d	-72.3	-73.8	-75.7	-77.9	-80.2
	2s	-71.6	-73.0	-74.9	-77.1	-79.5
${}^{208}_{\eta_b}\text{Pb}$	1f	-70.2	-71.7	-73.6	-75.8	-78.1
	1s	-72.8	-74.2	-76.1	-78.2	-80.5
	1p	-72.3	-73.7	-75.6	-77.7	-80.0
	1d	-71.3	-72.8	-74.6	-76.7	-79.0
${}^{208}_{\eta_b}\text{Pb}$	2s	-70.7	-72.1	-74.0	-76.1	-78.4
	1f	-70.2	-71.7	-73.5	-75.6	-77.9
	1s	-74.7	-76.2	-78.1	-80.3	-82.6
	1p	-74.2	-75.7	-77.5	-79.7	-82.1
${}^{208}_{\eta_b}\text{Pb}$	1d	-73.2	-74.7	-76.6	-78.8	-81.1
	2s	-72.7	-74.1	-76.0	-78.2	-80.5
	1f	-72.1	-73.6	-75.5	-77.6	-80.0

single-particle energies. From Tables I and II, we see that the bound-state energies for the η_b are larger than those of the Υ for the same nuclei and range of cutoff values explored. As before, these differences are probably due to two reasons: (a) The couplings $g_{\eta_b BB^*}$ and $g_{\Upsilon BB}$ are very different. Indeed, the results obtained in Ref. [45] on the η_c nuclear bound-state energies are closer to those the J/Ψ when the SU(4) flavor symmetry is broken, such that $g_{\eta_c DD^*} = (0.6/\sqrt{2})g_{J/\Psi DD} \simeq 0.424 g_{J/\Psi DD}$ [45,63]. Thus a reduced coupling $g_{\eta_b BB^*}$ can bring the η_b nuclear bound-state energies closer to those of the Υ , since the η_b self-energy is proportional to $g_{\eta_b BB^*}^2$. (b) The form factors are not equal for the vertices ΥBB and $\eta_b BB^*$ and we have to readjust the cutoff values, which means $\Lambda_B \neq \Lambda_{B^*}$, and the comparisons for the mass shifts have to be made for different values for the cutoff parameters.

IV. SUMMARY AND DISCUSSION

We have calculated the Υ - and η_b -nucleus bound-state energies for various nuclei neglecting any possible effects of the widths and various values of the cutoff parameter Λ_B that was introduced to regularize the divergent integral in the self-energies for these mesons. The bottomonium h -nucleus potentials were calculated using a local density approximation, with the inclusion of the BB (BB^*) meson loop in the Υ (η_c) self-energy. The nuclear density distributions and the in-medium B and B^* meson masses were calculated using the quark-meson coupling model. Using the bottomonium h potentials in nuclei, we have solved the Klein-Gordon equation and obtained bottomonium h -nucleus bound-state energies.

Our results show that the Υ and η_b mesons are expected to form bound states with all the nuclei studied, independent of the value of the cutoff parameter Λ_B . However, the particular values for the bound-state energies are dependent on cutoff parameter Λ_B . The sensitivity of our results to the cutoff parameter Λ_B has also been explored. However, a study needs to be done where we use a more properly determined coupling $g_{\eta_b BB^*}$ and different functional forms for the form factors. Furthermore, it is certainly necessary to include the possible effects of the widths for the Υ and η_b . Such elaborated studies are underway and will be reported elsewhere.

ACKNOWLEDGMENTS

We thank Prof. Tomoi Koide for useful conversations. G.N.Z. was supported in part by the Coordenação de Aperfeiçoamento de Pessoal de Nível Superior- Brazil (CAPES), and K.T. was supported by the Conselho Nacional de Desenvolvimento Científico e Tecnológico (CNPq) Process. No. 313063/2018-4 and No. 426150/2018-0, and Fundação de Amparo à Pesquisa do Estado de São Paulo (FAPESP) Process. No. 2019/00763-0, and this work was also part of the projects Instituto Nacional de Ciência e Tecnologia—Nuclear Physics and Applications (INCT-FNA), Brazil, Process. No. 464898/2014-5.

-
- [1] S. J. Brodsky, I. Schmidt, and G. F. de Teramond, *Phys. Rev. Lett.* **64**, 1011 (1990).
- [2] A. Hosaka, T. Hyodo, K. Sudoh, Y. Yamaguchi, and S. Yasui, *Prog. Part. Nucl. Phys.* **96**, 88 (2017).
- [3] G. Krein, in *XITH Conference on Quark Confinement and Hadron Spectrum*, edited by A. Andrianov, N. Brambilla, V. Kim, and S. Kolevatov, AIP Conf. Proc. No. 1701 (AIP, New York, 2016), p. 020012.
- [4] V. Metag, M. Nanova, and E. Y. Paryev, *Prog. Part. Nucl. Phys.* **97**, 199 (2017).
- [5] G. Krein, A. W. Thomas, and K. Tsushima, *Prog. Part. Nucl. Phys.* **100**, 161 (2018).
- [6] S. H. Lee and C. M. Ko, *Phys. Rev. C* **67**, 038202 (2003).
- [7] G. Krein, A. W. Thomas, and K. Tsushima, *Phys. Lett. B* **697**, 136 (2011).
- [8] K. Tsushima, D. H. Lu, G. Krein, and A. W. Thomas, *Phys. Rev. C* **83**, 065208 (2011).
- [9] K. Tsushima, D. Lu, G. Krein, and A. W. Thomas, in *T(R)opical QCD II Workshop*, edited by A. Kzlersü and A. W. Thomas, AIP Conf. Proc. No. 1354 (AIP, New York, 2011), p. 39.
- [10] G. Krein, *J. Phys.: Conf. Ser.* **422**, 012012 (2013).
- [11] F. Klingl, S. S. Kim, S. H. Lee, P. Morath, and W. Weise, *Phys. Rev. Lett.* **82**, 3396 (1999); **83**, 4224(E) (1999).
- [12] A. Hayashigaki, *Prog. Theor. Phys.* **101**, 923 (1999).
- [13] A. Kumar and A. Mishra, *Phys. Rev. C* **82**, 045207 (2010).
- [14] V. Belyaev, N. Shevchenko, A. Fix, and W. Sandhas, *Nucl. Phys. A* **780**, 100 (2006).
- [15] A. Yokota, E. Hiyama, and M. Oka, *Prog. Theor. Exp. Phys.* **2013**, 113D01 (2013).
- [16] M. E. Peskin, *Nucl. Phys. B* **156**, 365 (1979).
- [17] D. Kharzeev, *Proc. Int. Sch. Phys. Fermi* **130**, 105 (1996).
- [18] A. B. Kaidalov and P. E. Volkovitsky, *Phys. Rev. Lett.* **69**, 3155 (1992).
- [19] M. E. Luke, A. V. Manohar, and M. J. Savage, *Phys. Lett. B* **288**, 355 (1992).
- [20] G. F. de Teramond, R. Espinoza, and M. Ortega-Rodriguez, *Phys. Rev. D* **58**, 034012 (1998).
- [21] S. J. Brodsky and G. A. Miller, *Phys. Lett. B* **412**, 125 (1997).
- [22] A. Sibirtsev and M. B. Voloshin, *Phys. Rev. D* **71**, 076005 (2005).
- [23] M. B. Voloshin, *Prog. Part. Nucl. Phys.* **61**, 455 (2008).
- [24] J. Tarrús Castellà, and G. Krein, *Phys. Rev. D* **98**, 014029 (2018).
- [25] K. Yokokawa, S. Sasaki, T. Hatsuda, and A. Hayashigaki, *Phys. Rev. D* **74**, 034504 (2006).
- [26] L. Liu, H. W. Lin, and K. Orginos, *PoS LATTICE2008*, 112 (2008).
- [27] T. Kawanai and S. Sasaki, *Phys. Rev. D* **82**, 091501(R) (2010).
- [28] T. Kawanai and S. Sasaki, *PoS LATTICE2010*, 156 (2010).
- [29] U. Skerbis and S. Prelovsek, *Phys. Rev. D* **99**, 094505 (2019).
- [30] S. R. Beane, E. Chang, S. D. Cohen, W. Detmold, H. W. Lin, K. Orginos, A. Parreño, and M. J. Savage, *Phys. Rev. D* **91**, 114503 (2015).
- [31] M. Albeti, G. S. Bali, S. Collins, F. Knechtli, G. Moir, and W. Soldner, *Phys. Rev. D* **95**, 074501 (2017).
- [32] A. Ali *et al.* (GlueX Collaboration), *Phys. Rev. Lett.* **123**, 072001 (2019).
- [33] M. Durante, P. Indelicato, B. Jonson, V. Koch, K. Langanke, U. G. Meißner, E. Nappi, T. Nilsson, T. Stöhlker, E. Widmann, and M. Wiescher, *Phys. Scr.* **94**, 033001 (2019).
- [34] R. Aaij *et al.* (LHCb Collaboration), *Eur. Phys. J. C* **80**, 191 (2020).
- [35] Tichouk, H. Sun, and X. Luo, *Phys. Rev. D* **101**, 094006 (2020).
- [36] Tichouk, H. Sun, and X. Luo, *Phys. Rev. D* **101**, 054035 (2020).
- [37] V. P. Goncalves and B. D. Moreira, *Phys. Rev. D* **97**, 094009 (2018).
- [38] S. R. Klein, *Phys. Rev. D* **98**, 118501 (2018).
- [39] Y. Xu, Y. Xie, R. Wang, and X. Chen, *Eur. Phys. J. C* **80**, 283 (2020).
- [40] O. Gryniuk, S. Joosten, Z. E. Meziani, and M. Vanderhaeghen, *Phys. Rev. D* **102**, 014016 (2020).
- [41] R. Aaij *et al.* (LHCb Collaboration), *J. High Energy Phys.* **11** (2018) 194.
- [42] W. Liang, N. Ikeno, and E. Oset, *Phys. Lett. B* **803**, 135340 (2020).
- [43] C. M. Ko, P. Levai, X. J. Qiu, and C. T. Li, *Phys. Rev. C* **45**, 1400 (1992).
- [44] M. Asakawa, C. M. Ko, P. Levai, and X. J. Qiu, *Phys. Rev. C* **46**, R1159 (1992).
- [45] J. J. Cobos-Martínez, K. Tsushima, G. Krein, and A. W. Thomas, *Phys. Lett. B* **811**, 135882 (2020).
- [46] G. N. Zeminiani, J. J. Cobos-Martínez, and K. Tsushima, *Eur. Phys. J. A* **57**, 259 (2021).
- [47] P. A. M. Guichon, *Phys. Lett. B* **200**, 235 (1988).
- [48] K. Tsushima and F. Khanna, *Phys. Lett. B* **552**, 138 (2003).
- [49] K. Tsushima, K. Saito, A. W. Thomas, and S. V. Wright, *Phys. Lett. B* **429**, 239 (1998); **436**, 453(E) (1998).
- [50] P. A. M. Guichon, K. Saito, E. N. Rodionov, and A. W. Thomas, *Nucl. Phys. A* **601**, 349 (1996).

- [51] K. Saito, K. Tsushima, and A. W. Thomas, *Nucl. Phys. A* **609**, 339 (1996).
- [52] K. Tsushima, *Assoc. Asia Pac. Phys. Soc.* **29**, 37 (2019).
- [53] K. Saito, K. Tsushima, and A. W. Thomas, *Prog. Part. Nucl. Phys.* **58**, 1 (2007).
- [54] P. A. M. Guichon, *Nucl. Phys. A* **497**, 265C (1989).
- [55] J. R. Stone, P. A. M. Guichon, P. G. Reinhard, and A. W. Thomas, *Phys. Rev. Lett.* **116**, 092501 (2016).
- [56] Z. W. Lin and C. M. Ko, *Phys. Lett. B* **503**, 104 (2001).
- [57] Z. W. Lin and C. M. Ko, *Phys. Rev. C* **62**, 034903 (2000).
- [58] J. J. Cobos-Martínez, K. Tsushima, G. Krein, and A. W. Thomas, *Phys. Lett. B* **771**, 113 (2017).
- [59] J. J. Cobos-Martínez, K. Tsushima, G. Krein, and A. W. Thomas, *Phys. Rev. C* **96**, 035201 (2017).
- [60] J. J. Cobos-Martínez, K. Tsushima, G. Krein, and A. W. Thomas, *J. Phys.: Conf. Ser.* **912**, 012009 (2017).
- [61] J. J. Cobos-Martínez, K. Tsushima, G. Krein, and A. W. Thomas, PoS **Hadron2017**, 209 (2018).
- [62] J. J. Cobos-Martínez, K. Tsushima, G. Krein, and A. W. Thomas, *JPS Conf. Proc.* **26**, 024033 (2019).
- [63] W. Lucha, D. Melikhov, H. Sazdjian, and S. Simula, *Phys. Rev. D* **93**, 016004 (2016); **93**, 019902(E) (2016).
- [64] K. Saito, K. Tsushima, and A. W. Thomas, *Phys. Rev. C* **56**, 566 (1997).